

# Numerical Heat Transfer, Part B: Fundamentals

## An International Journal of Computation and Methodology

ISSN: (Print) (Online) Journal homepage: [www.tandfonline.com/journals/unhb20](http://www.tandfonline.com/journals/unhb20)

## Analytical investigation on energy separation in Ranque–Hilsch vortex tube

**Karthik A. V. & Vighnesha Nayak**

To cite this article: **Karthik A. V. & Vighnesha Nayak** (2021) Analytical investigation on energy separation in Ranque–Hilsch vortex tube, Numerical Heat Transfer, Part B: Fundamentals, 80:5-6, 136-154, DOI: [10.1080/10407790.2021.1969816](https://doi.org/10.1080/10407790.2021.1969816)

To link to this article: <https://doi.org/10.1080/10407790.2021.1969816>



Published online: 08 Sep 2021.



Submit your article to this journal [↗](#)



Article views: 234



View related articles [↗](#)



View Crossmark data [↗](#)



Citing articles: 3 View citing articles [↗](#)



# Analytical investigation on energy separation in Ranque–Hilsch vortex tube

Karthik A. V. and Vighnesha Nayak

Department of Mechanical Engineering, A. J. Institute of Engineering and Technology, Mangalore, Karnataka, India

## ABSTRACT

A vortex tube is a simple device with no moving parts that has the inherent capability of separating the high pressure inlet stream into two low pressure outlet streams. One of the outlet streams is the peripheral stream that has higher temperature than the inlet while the other outlet stream is the inner or core stream that has temperature lower than the inlet. Various theories have been put forwarded by many investigators to explain the mechanism of this temperature separation in vortex tube. This article deals with the analytical approach to calculate the amount of heat transfer between the core and the peripheral streams. In the process, we have established an empirical relationship between the length of the vortex tube and the surface that divides the cold and the hot flows, proceeding in the opposite directions through the tube. We have also derived the dependence of heat transfer on the length of the vortex tube keeping the diameter of the vortex tube constant. The necessary boundary conditions needed for the analysis are obtained from CFD analysis.

## ARTICLE HISTORY

Received 9 July 2021  
Accepted 30 July 2021

## KEYWORDS

CFD; energy separation;  
mathematical model;  
vortex tube

## 1. Introduction

A vortex tube is a simple device with no moving parts that has the inherent capability of separating the high pressure inlet stream into two low pressure outlet streams. One of the outlet streams is the peripheral stream that has higher temperature than the inlet while the other outlet stream is the inner or core stream that has temperature lower than the inlet.

The schematic of a typical vortex tube is shown in [Figure 1](#). It is basically a hollow cylinder with three terminals. The inlet, terminal-1 is tangential to the tube. The inlet is subjected to pressurized fluid. The fluid enters the tube tangentially and starts swirling at a very high rotational velocity while moving toward terminal-2 (hot end) thus creating the outer vortex. So at any point, the fluid has two velocity components, the swirling velocity and the axial velocity. At terminal-2, there is a conical valve. Due to the presence of the valve the effective annular space is significantly smaller than the cross section area of the tube. This small outlet can't accommodate the entire swirling mass flow through the tube. As a result only a small part of the original flow goes out through this port, the rest of the flow "bounces" back and creates a counter flow, moving toward terminal-3 (cold end). This counter flow forms the inner vortex which has a radius smaller than the outer vortex. The centre-line of both the vortices remains aligned with the axis of the tube itself. The entire process is pictorially represented in [Figure 2](#).

### Nomenclature

|  |   |                          |   |
|--|---|--------------------------|---|
| D                                      | diameter of the vortex tube   | $\dot{Q}_{\text{total}}$ | total heat transfer   |
| d                                      | $\dot{Q}$ heat transfer for a differential element                    | $R_b$                    | distance of the contact surface between hot and cold flow from the axis of the tube |
| $k_t$                                  | turbulent thermal conductivity  |                          |   |
| L                                      | length of the vortex tube   | R                        | location of a point along radial direction measured from the axis of the tube       |
| L                                      | location of a point along the length of the tube, measured from inlet |                          |   |
| M, N, R, F,                            |   | T                        | temperature   |
| $r', f, \alpha, \beta, \gamma, \delta$ | constants   | $\mu$                    | hot mass fraction   |
| P                                      | a constant in the range 0 to 1  |                          |   |

Now, due to the pressure gradient in the radial and axial direction, the inner flow expands and the outer vortex gets compressed which is one of the theories [1] that explains the energy transfer that takes place between the inner and the outer vortices through their contact surface. Heat flows from the core toward the periphery. As a result the outer vortex heats up by absorbing energy from the inner vortex and the inner vortex cools down by dissipating energy. The magnitude of the heat transfer depends on various geometric parameters such as length and diameter of the tube, diameter of the orifice as well as operating parameters such as inlet pressure, ratio of the mass flow rates between terminal-2 and terminal-1. Various theories have been put forward by many investigators to explain the mechanism of this temperature separation in vortex tube. The physical phenomenon of temperature separation inside a vortex tube was first discovered by George Joseph. Ranque in 1930 [1]. He suggested that the energy separation takes place due to simultaneous effect of compression and expansion. Later the effect of multiple geometric parameters on the performance of vortex tube was investigated by R. Hilsch [2] and he stated that the internal friction between the different layers of the working fluid also takes part in the energy separation phenomenon. Kurosaka [3,4] demonstrated that the acoustic streaming induced by orderly disturbances within the swirling flow is the cause for energy separation. In this article, for the first time, we present a novel method to analytically calculate the amount of heat transfer between the inner vortex and the outer vortex. We have also established the dependence of the heat transfer on the length of the vortex tube while keeping other parameters constant.

## 2. Heat energy calculation (analytical approach)

### 2.1. Stagnation point

Usually the presence of an obstruction in the flow field generates a particular point before the obstruction where the local velocity of the flow reduces to zero. This is known as the stagnation point. In vortex tube the stagnation point has immense significance primarily because at this point flow reversal takes place due to: (a) the presence of the conical valve which acts as obstruction and (b) the pressure gradient in the axial direction.

The fluid particles, moving forward toward terminal-2, in the vicinity of the axis of the tube, gradually lose momentum and eventually change their direction toward terminal-3. After the stagnation point, the inner vortex does not exist. Hence, no energy transfer takes place after the stagnation point. The schematic representation of the stagnation point is shown in Figure 3.

As shown in Figure 4 the entire length of the vortex tube is L measured from terminal-1 along the axis. Let,  $l$  be the distance of the stagnation point measured from inlet of the vortex tube. So, we can write,

$$l = pL \quad (1)$$

where,  $0 < p < 1$ .

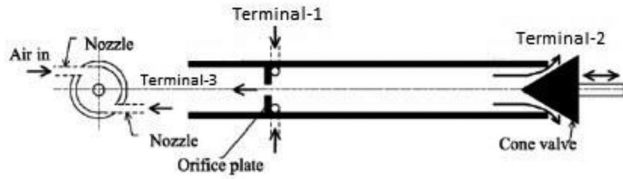


Figure 1. Cross-sectional view of a vortex tube.

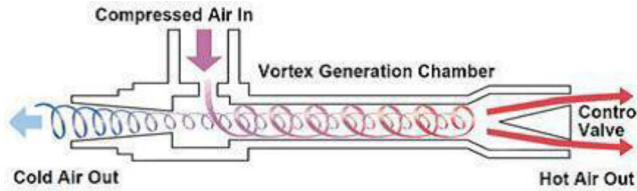


Figure 2. Working process.

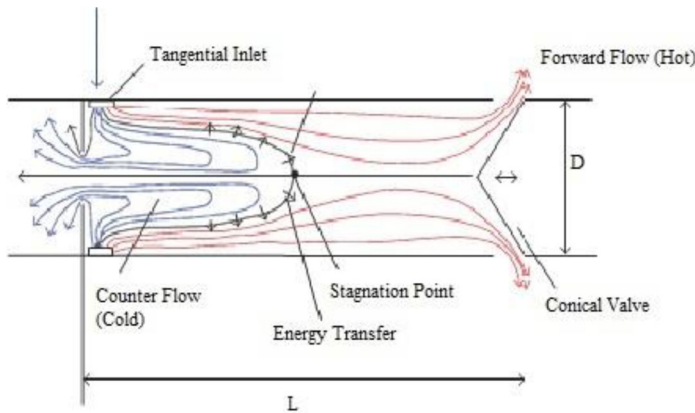


Figure 3. Effect of stagnation point.

**2.2. Equation of “contact surface” in 2-D interpretation**

In this article by ‘contact surface’ we refer the surface of contact between the outer vortex and the inner vortex through which the energy transfer takes place. Figure shows the 2D representation of the contact surface inside the typical vortex tube.

$R_b(l)$  represents the function that defines the distance between the contact surface and the axis of the tube. As shown in Figure 5, the value of  $R_b$  is not constant for different values of  $l$ . More specifically the value of  $R_b$  decreases steadily as we move toward terminal-2 from the inlet (terminal-1).

Let us further assume that the function  $R_b(l)$  can be approximated by an exponentially decreasing function of  $l$  i.e.,

$$R_b(l) = Re^{-\alpha l} \tag{2}$$

Equation (2) represents the equation of the contact line in the first quadrant, shown in red, in Figure 5.

**2.3. Equation of the rate of change of temperature in radial direction**

Inside the vortex tube, at each cross section, there is a temperature distribution from the core to the periphery. We are interested to find out the rate of change of temperature at the contact

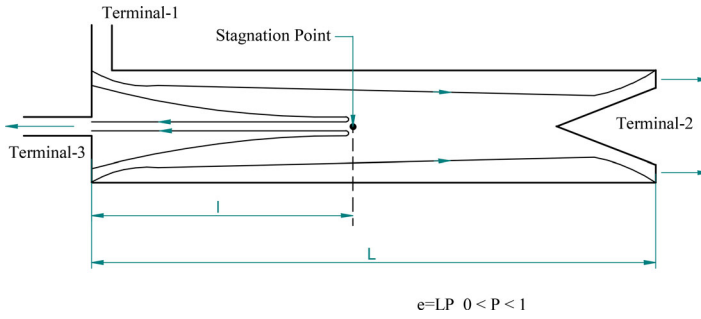


Figure 4. Location of the stagnation point.

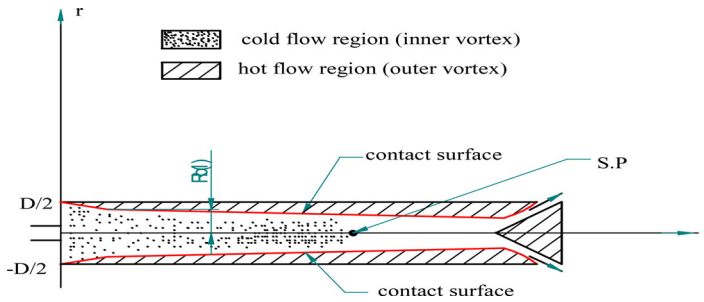


Figure 5. Contact surface between cold and hot flow.

surface and also to find out the variation of the rate of change of temperature at the contact surface with increasing values of  $l$ .

From the work of U. Behera et al. [5] it is clear that as we move from the inlet toward terminal-2, the temperature gradient gradually reduces and after the stagnation point it becomes null.

Now,  $\left\{ \left[ \frac{dT}{dr} \right]_{r=R_b} (l) \right\} = F(l)$  (say), represents the function that defines the relation between the radial temperature gradient at the contact line and the length  $l$ .

Let us further assume that  $F(l)$  can be approximated by a polynomial function i.e.,

$$F(l) = Al^4 + Bl^3 + Cl^2 + Dl + E \quad (3)$$

#### 2.4. Calculation of the heat transfer at a particular cross section

Suppose we want to calculate the heat energy transfer at particular cross section, located at a distance “ $a$ ” units away from the inlet. For this cross section the contact surface would be the shape of a ring of radius  $R_b$  ( $l = a$ ) =  $Re^{-\alpha a}$ .

Hence, the temperature gradient at the contact surface at a distance “ $a$ ” units from the inlet would be  $\left\{ \left[ \frac{dT}{dr} \right]_{r=R_b} (l = a) \right\} = F(l = a) = Aa^4 + Ba^3 + Ca^2 + Da + E$ .

The general heat transfer equation in a flow field is given as,

$$\dot{Q} = 2\pi r k_t \frac{dT}{dr} \quad (4)$$

So, the value of energy transfer at  $l = a$ , will be

$$\begin{aligned} \dot{q}_{l=a} &= 2\pi k_t \{R_b (l = a)\} \{F(l = a)\} \\ &= 2\pi k_t \{Re^{-\alpha a}\} \{Aa^4 + Ba^3 + Ca^2 + Da + E\}. \end{aligned}$$

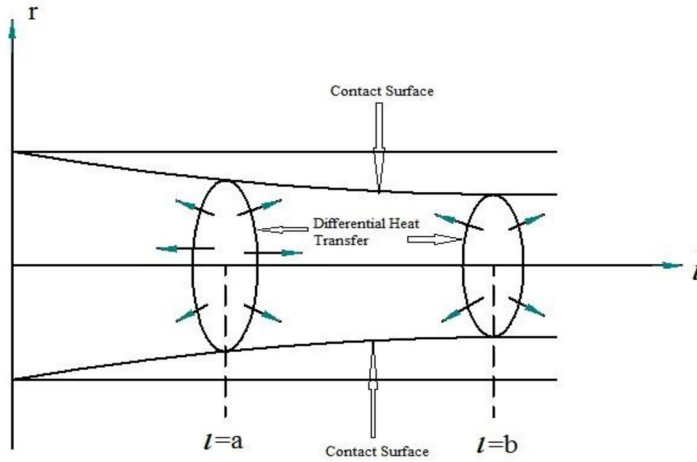


Figure 6. Heat transfer.

Again, if we want to calculate the value of heat transfer at  $l=b$ , we can proceed in the similar manner and find,

$$\begin{aligned} \dot{q}_{l=b} &= 2\pi k_t \{R_b(l=b)\} \{F(l=b)\} \\ &= 2\pi k_t \{Re^{-\alpha b}\} \{Ab^4 + Bb^3 + Cb^2 + Db + E\}. \end{aligned}$$

The entire process is depicted in Figure 6.

### 2.5. Calculation of transfer in the entire tube

The total heat transfer across the contact surface in the entire tube can be calculated by summing up the heat transfer of all the differential cross section elements till the stagnation point.

$$\begin{aligned} \dot{Q}_{Total} &= \dot{q}_{l=a} + \dot{q}_{l=b} + \dots + (q_{l=pL}) \\ \dot{Q}_{Total} &= 2\pi k_t \int_0^{pL} \{R_b(l)\} \{F(l)\} dl \\ &= 2\pi k_t \int_0^{pL} \{Re^{-\alpha l}\} \{Al^4 + Bl^3 + Cl^2 + Dl + E\} dl \end{aligned} \tag{5}$$

### 2.6. Calculation of the function $R_b(l)$

As the vortex tube is symmetrical about the axis, instead of considering the entire cross section area at a distance  $l=a$ , let us focus on the first quadrant. The general profile of the curve between the radial distance and the axial velocity is shown Figure 7.

The region above the  $V_x = 0$  line would be outer vortex region and region below the line would be the inner vortex region. The  $V_x = 0$  line intersects the curve at point  $P$  and the  $X$  coordinate of point  $P$  is the value of  $R_b$  at  $l=a$ .

In the same way one can calculate the values of  $R_b$  in different cross section areas along the length of the tube and form an empirical relationship between  $R_b$  and  $l$ .

For our calculation, the graphs between radial distance and axial velocity, at different cross section areas along the length are plotted through CFD analysis.

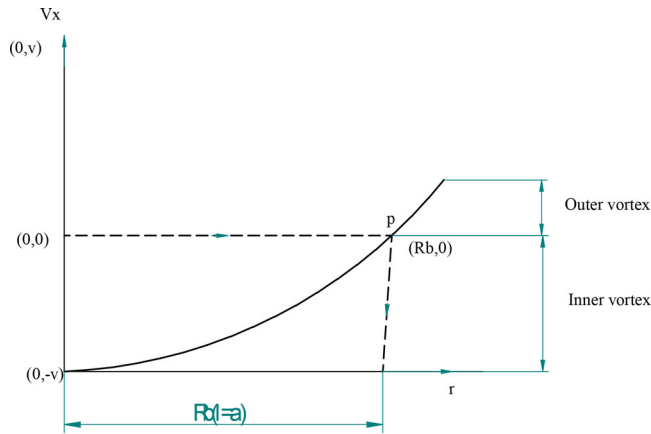
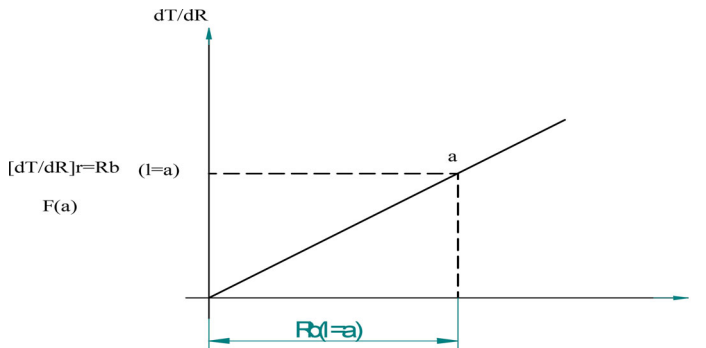


Fig-7

**Figure 7.** Variation of axial velocity with radial distance.

**Figure 8.** Variation of radial temperature gradient with radial distance.

## 2.7. Calculation of the function $F(l) \left( = \left[ \frac{dT}{dr} \right]_{r=R_b} (l) \right)$

As the vortex tube is symmetrical about the axis, instead of considering the entire cross section area at a distance  $l = a$ , let us focus on the first quadrant. Figure 8 represents the graph of the gradient of radial temperature distribution along the radius of the tube.

Now, at this point we know the value of  $R_b$  ( $l = a$ ). We can locate that point on the X axis, project it on to the curve as shown in Figure 8. The Y co-ordinate of point Q would be function  $F$  at  $l = a$ .

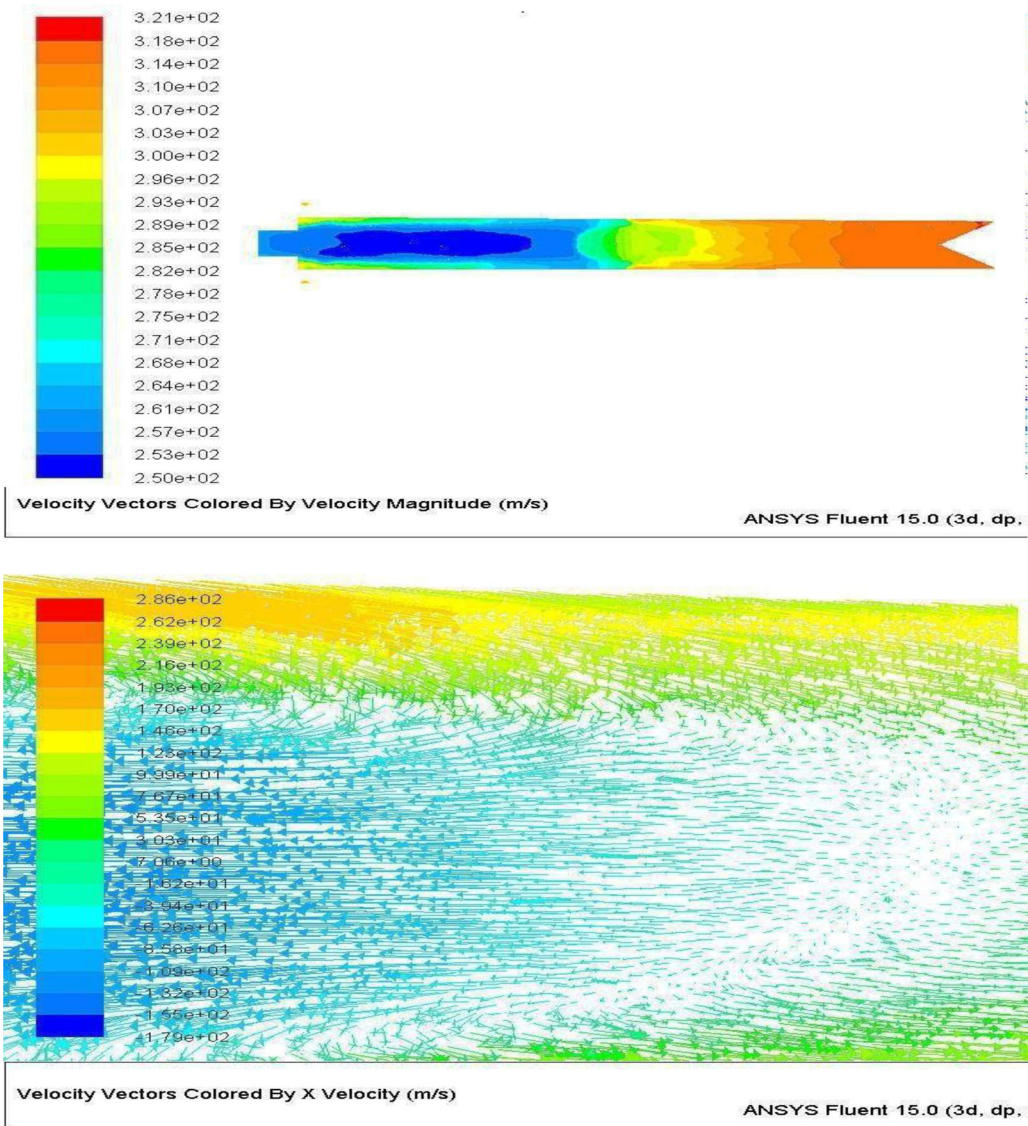
In similar manner, we can calculate the values of  $F$  in different cross section areas along the length of the tube and form an empirical relationship between  $F$  and  $l$ .

For our calculation, the graphs of the gradient of radial temperature distribution and radial distance, at different cross section areas along the length are plotted through CFD analysis.

## 3. Heat energy calculation (numerical approach)

### 3.1. CFD specifications

CFD Analysis of a vortex tube with 12 mm diameter has been carried out in ANSYS FLUENT15. 3-D modeling and meshing of the vortex tube is done in GAMBIT 2.4.6 with mesh interval size 0.6 mm, Tet/Hybrid grid mesh with number of elements equals to 1556304 for  $L/D = 30$  vortex tube and with mesh elements equals to 522323 for  $L/D = 10$  is used for analysis. Mesh interval size of

(a) Stagnation region of  $L/D=10$ 

**Figure 9.** CFD results of vortex tube with  $L/D = 10$ .

0.6 mm gives rise to maximum energy separation with less analysis time. Vortex tube model has been done by using six convergent nozzles with 1.1 mm diameter. Density based analysis using  $k-\epsilon$  RNG model with air as ideal gas, second order upwind scheme is used for analysis.

Important CFD results on location of stagnation point, velocity profile and temperature distribution are represented in **Figures 9** and **10**.

### 3.2. Vortex tube with $L/D = 10$

Vortex tube with the following parameters has been modeled as shown in **Figure 11**. The parameters include: diameter of vortex tube,  $D = 12$  mm,  $L/D = 10$ , type of fluid: Air, inlet pressure: 6 bar, cold outlet pressure = 1.3 bar, hot outlet pressure = 1 bar,  $\mu = 0.1$ .

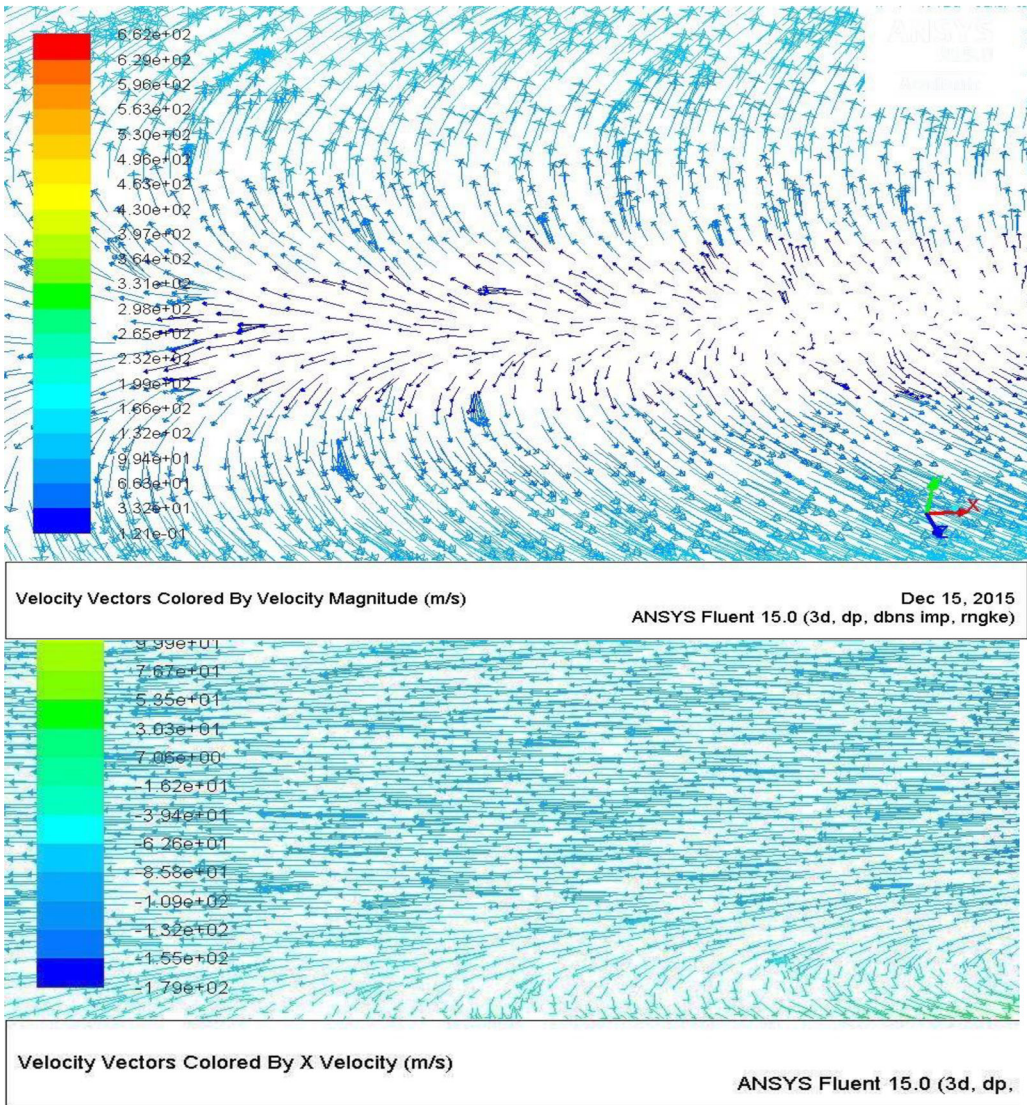
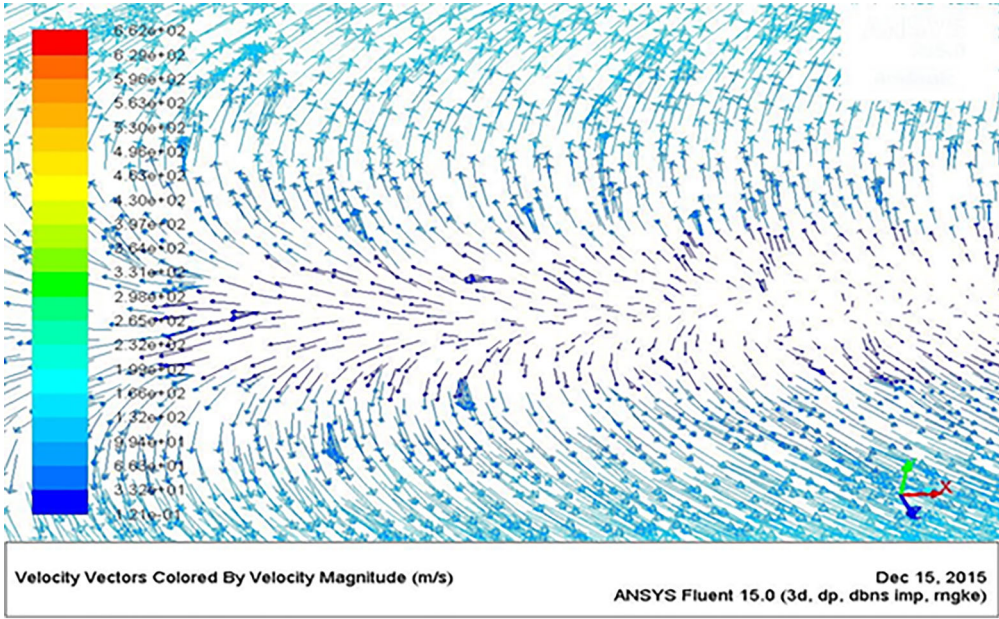
(b) Temperature separation for  $L/D=10$ 

 (c) Velocity profile before stagnation point of  $L/D=10$ 

Figure 9. (Continued).

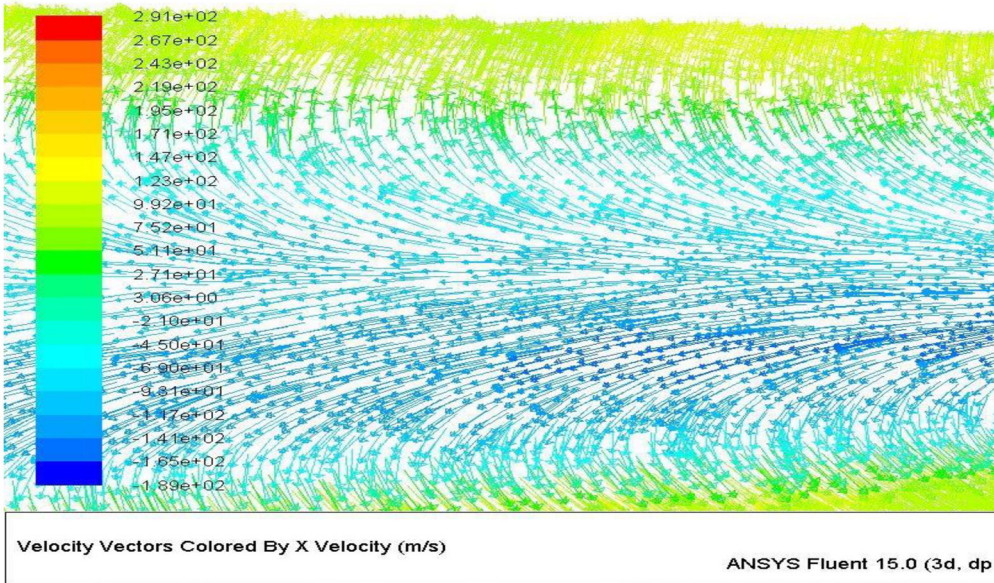
### 3.2.1. Calculation of $R_b(l)$

Figure 12 shows the variation  $R_b$  at of various cross sections along the length of the vortex tube. The variation of  $R_b$  along the length of VT  $l$  is given in Table 1 and is represented in Figure 13. From the graph plotted in Figure 13, we get the empirical relationship between  $R_b(l)$  and  $l$  as,

$$R_b(l) = 3.6384e^{-0.013l} \quad (6)$$



(a) Stagnation region of  $L/D=30$



(b) Temperature separation for  $L/D=30$

Figure 10. CFD results of vortex tube with  $L/D = 30$ .

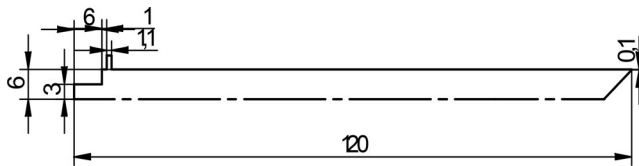


Figure 11. Dimensions of vortex tube model with  $L/D = 10$ .

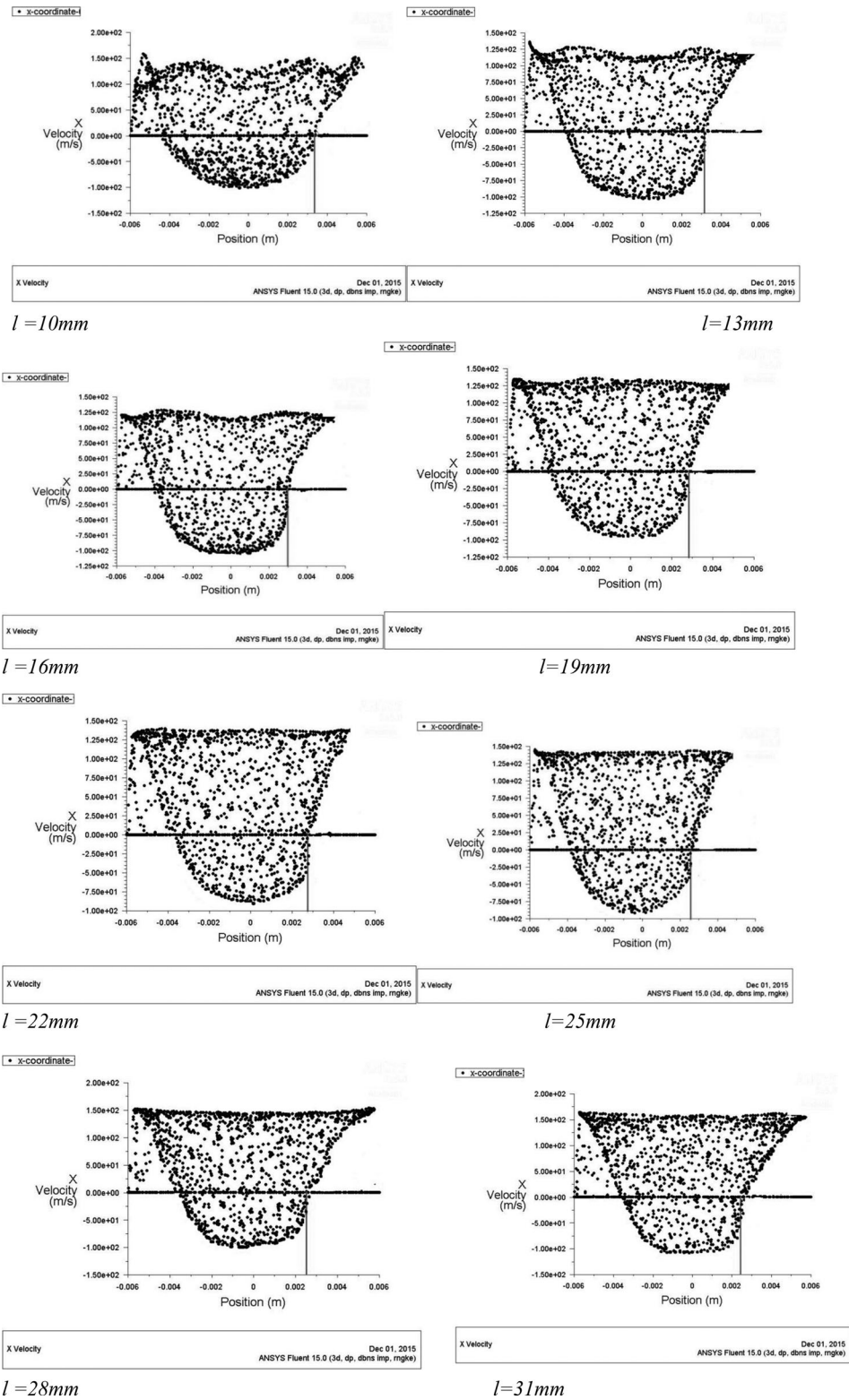


Figure 12. Variation of axial velocity with radial distance at different cross sections for  $L/D = 10$ .

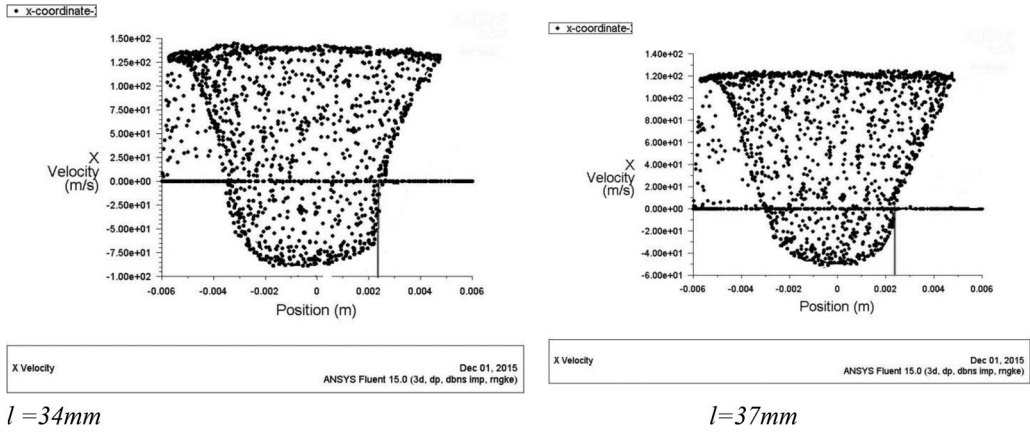


Figure 12. (Continued).

Table 1. Values of  $R_b$  at different cross sections along the length of VT for  $L/D = 10$ .

| Position( $l$ ), mm | $R_b(l)$ , mm |
|---------------------|---------------|
| 8                   | 3.3           |
| 10                  | 3.2           |
| 13                  | 3.05          |
| 16                  | 2.95          |
| 19                  | 2.82          |
| 22                  | 2.75          |
| 25                  | 2.6           |
| 28                  | 2.53          |
| 31                  | 2.45          |
| 34                  | 2.35          |
| 37                  | 2.25          |
| 40                  | 2.2           |

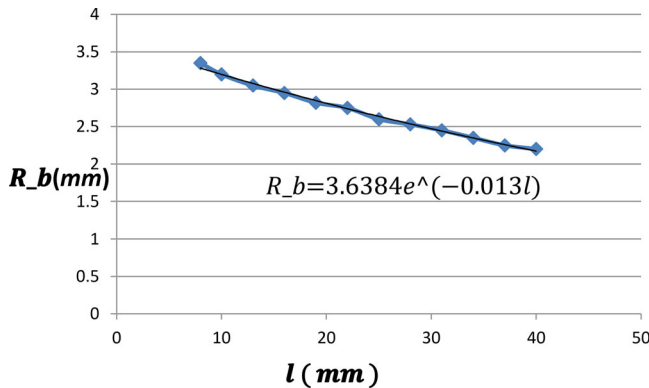


Figure 13. Empirical equation of contact surface for  $L/D = 10$ .

### 3.2.2. Calculation of $F(l)$ $\left( = \left[ \frac{dT}{dr} \right]_{r=R_b}(l) \right)$

Figure 14 shows gradient of radial temperature distribution versus the radial distance, at different cross sections along the length of the VT. The values of temperature gradients along the length are obtained from Figure 14 is show in Figure 15 and given in Table 2.

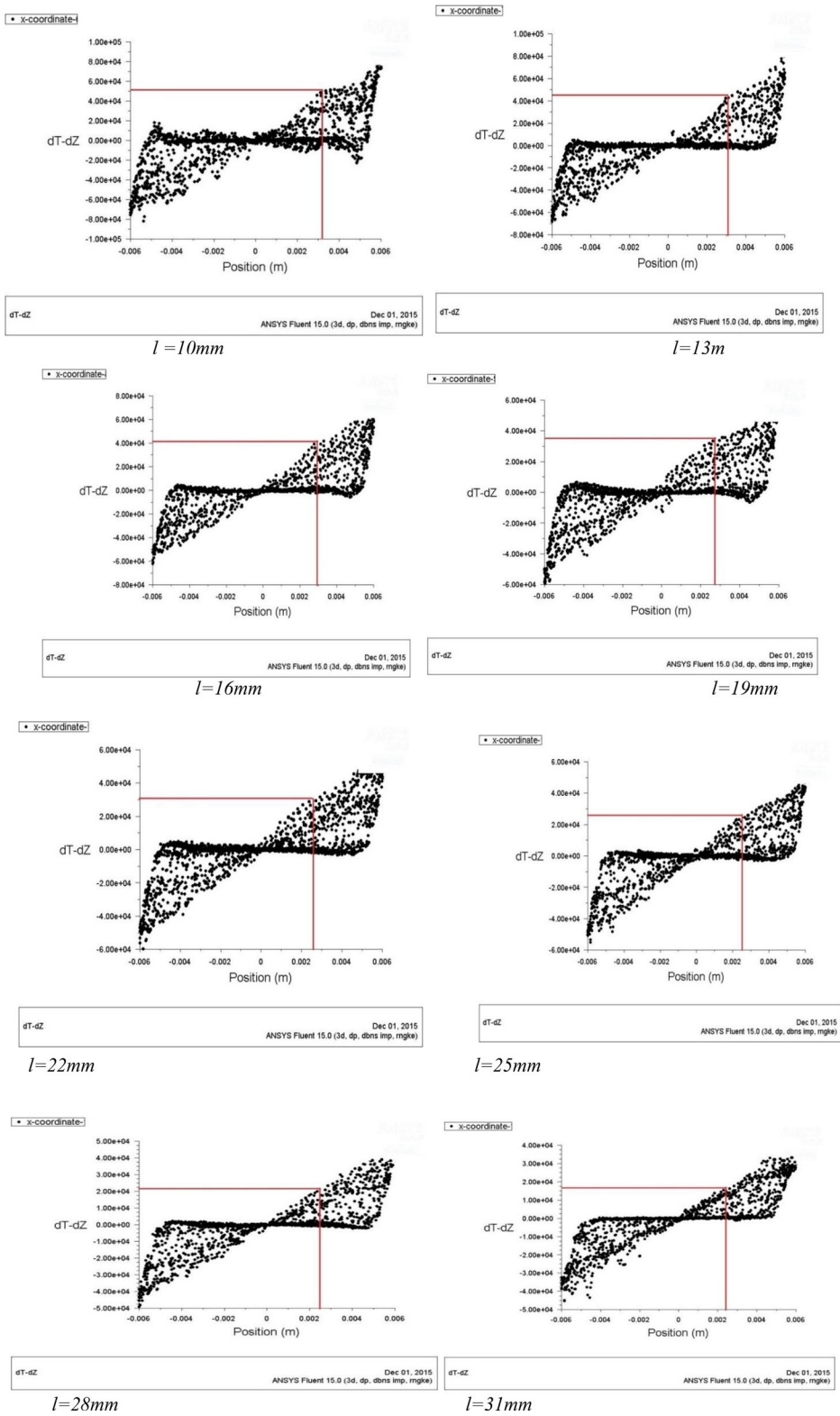


Figure 14. Variation of radial temperature gradient and radial distance at different cross sections for  $L/D = 10$ .

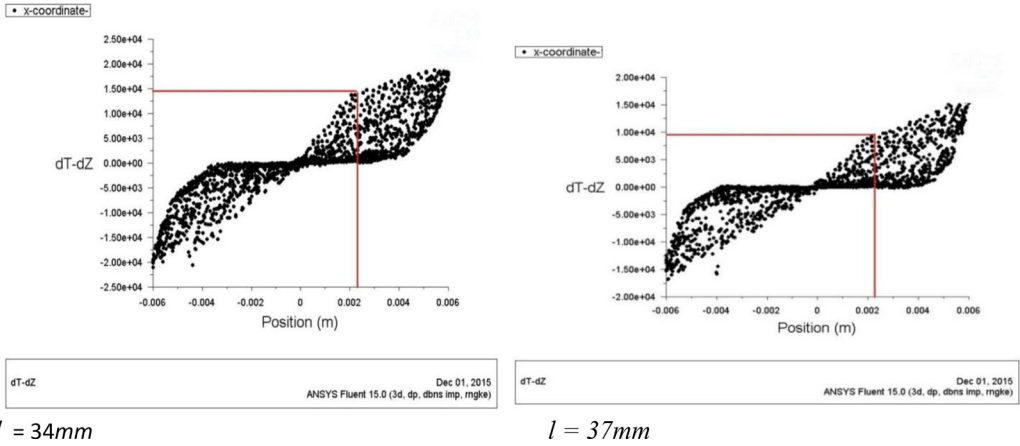


Figure 14. (Continued).

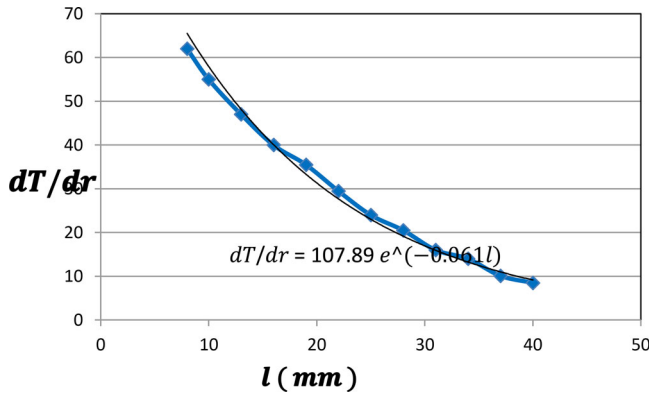


Figure 15. Empirical equation of radial temperature gradient for L/D = 10.

Table 2. Values of temperature gradient along the length of VT for L/D = 10.

| Position ( $l$ ), mm | $F(l)$ , K/mm |
|----------------------|---------------|
| 8                    | 61.0          |
| 10                   | 55.0          |
| 13                   | 47.0          |
| 16                   | 40.0          |
| 19                   | 35.5          |
| 22                   | 29.5          |
| 25                   | 24.0          |
| 28                   | 20.5          |
| 31                   | 16.0          |
| 34                   | 14.0          |
| 37                   | 10.1          |
| 40                   | 8.5           |

From the graph plotted in Figure 15, we get the empirical relationship between  $\frac{dT}{dr}$  and  $l$  as,

$$F(l) = 107.89e^{-0.061l} \tag{7}$$

### 3.2.3. Total heat transfer

The total heat transfer across the contact surface between the cold and the hot fluid over the length till the stagnation point of the VT will be,

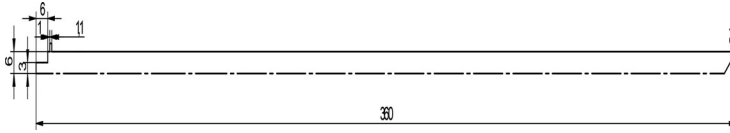


Figure 16. Dimensions of vortex tube model with  $L/D = 30$ .

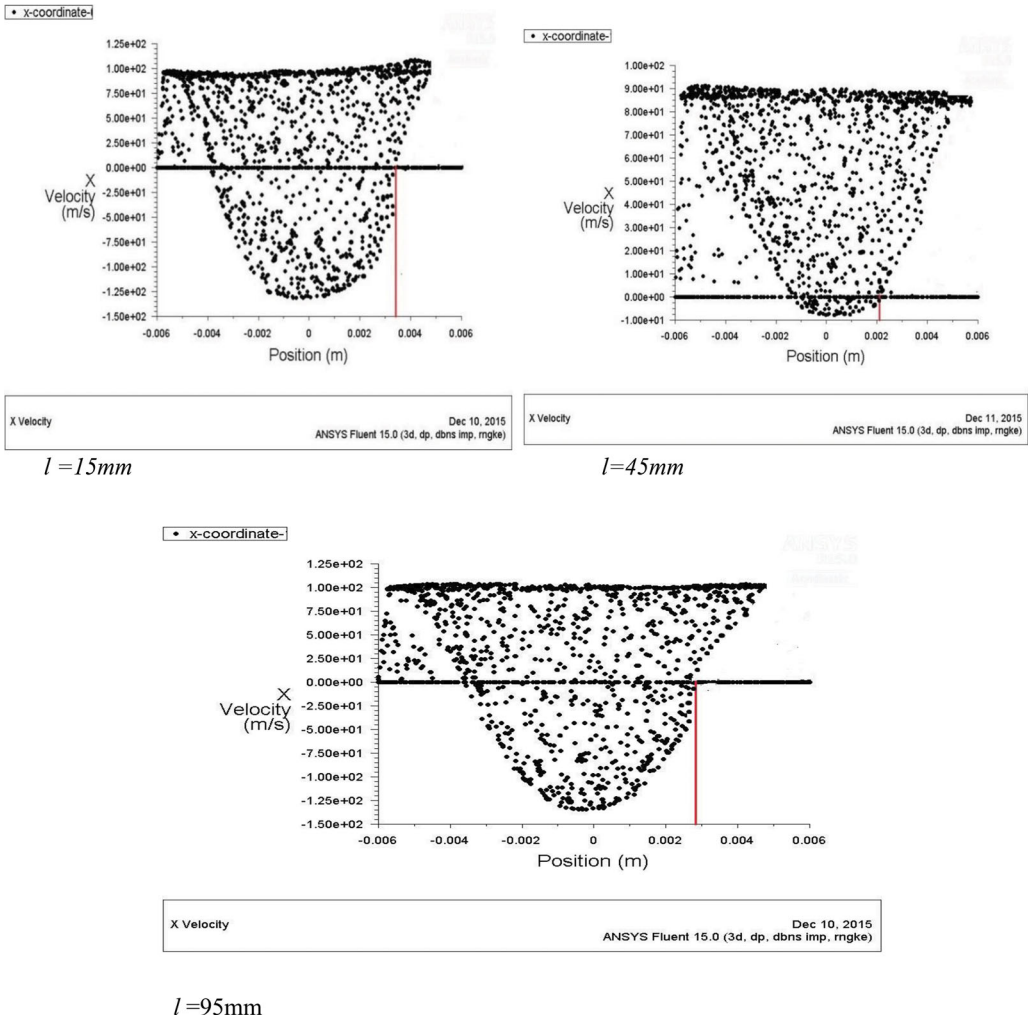
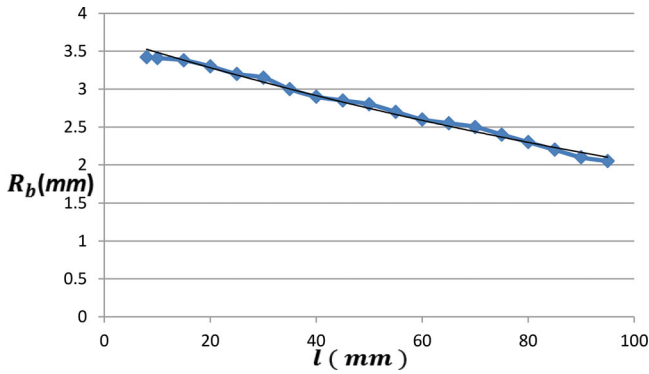


Figure 17. Variation of axial velocity with radial distance at different cross sections for  $L/D = 30$ .

$$\begin{aligned} \dot{Q}_{total} &= 2\pi k_t \int_{10}^{40} R_b(l) F(l) dl \text{ [for this model, inlet is at 10mm and stagnation point is at} \\ &\quad \text{40mm from cold end]} \\ &= (0.028) \int_{10}^{40} \{3.6384e^{-0.013l}\} \{107.89e^{-0.061l}\} dl \end{aligned}$$

**Table 3.** Values of  $R_b$  at different cross sections along the length of VT for  $L/D = 30$ .

| Position ( $l$ ) | $R_b(l)$ |
|------------------|----------|
| 8                | 3.44     |
| 10               | 3.42     |
| 15               | 3.4      |
| 20               | 3.3      |
| 25               | 3.2      |
| 30               | 3.15     |
| 35               | 3        |
| 40               | 2.9      |
| 45               | 2.85     |
| 50               | 2.8      |
| 55               | 2.7      |
| 60               | 2.6      |
| 65               | 2.55     |
| 70               | 2.5      |
| 75               | 2.4      |
| 80               | 2.3      |
| 85               | 2.2      |
| 90               | 2.15     |
| 95               | 2.05     |



**Figure 18.** Empirical equation of contact surface for  $L/D = 30$ .

$$\text{Where, } 2\pi k_t = 2\pi(0.045) = 0.028 = 74.47 \text{ Watt}$$

It may be noted that the value of the total heat transfer obtained by the present analytical method matches well with the total heat transfer value of 85.039 Watt obtained through CFD analysis for the same vortex tube of  $L/D = 10$ , by Behera et al. [5].

### 3.3. Vortex tube with $L/D = 30$

Vortex tube with the following parameters has been modeled as shown in Figure 16. The parameters include: diameter of vortex tube,  $D = 12$  mm,  $L/D = 30$ , type of fluid: Air, inlet pressure: 6 bar, cold outlet pressure = 1.3 bar, hot outlet pressure = 1 bar,  $\mu = 0.1$ .

#### 3.3.1. Calculation of $R_b(l)$

Figure 17 shows the variation of axial velocity versus radial distance at various cross sections along the length of the VT tube. The variation of  $R_b$  along the length of VT is given in Table 3, and is represented in Figure 18.

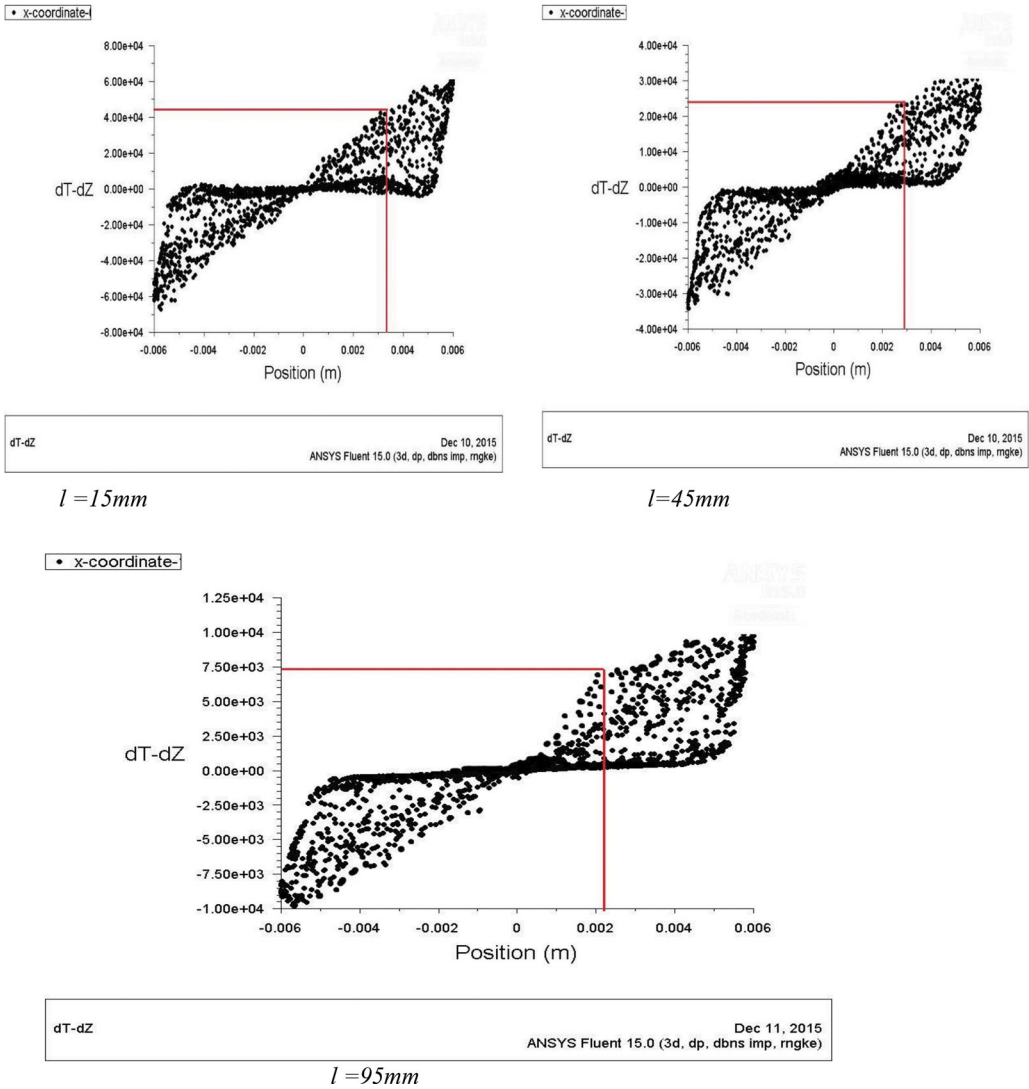


Figure 19. Variation of radial temperature gradient with radial distance at different cross sections for  $L/D = 30$ .

From the Figure 18, we get the empirical relationship between  $R_b(l)$  and  $l$  as,

$$R_b(l) = 3.05 e^{-0.009l} \quad (8)$$

### 3.3.2. Calculation of $F(l) (= \left[ \frac{dT}{dr} \right]_{r=R_b} (l))$

Figure 19 shows the gradient of radial temperature distribution versus the radial distance at different cross sections, along the length of VT. The values of temperature gradients along the length are obtained from Figure 19 is shown in Figure 20 and given in Table 4.

From the Figure 18, we get the empirical relationship

$$F(l) = 65.038e^{-0.048l} \quad (9)$$

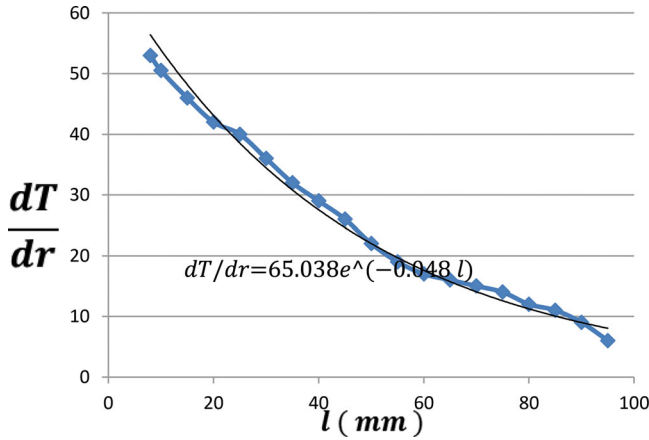


Figure 20. Empirical equation of radial temperature gradient for L/D = 30.

Table 4. Values of temperature gradient along the length of VT for L/D = 30.

| Position (l) | F(l) |
|--------------|------|
| 8            | 53   |
| 10           | 50   |
| 15           | 45   |
| 20           | 42   |
| 25           | 40   |
| 30           | 36   |
| 35           | 32   |
| 40           | 29   |
| 45           | 26   |
| 50           | 22   |
| 55           | 19   |
| 60           | 17   |
| 65           | 16   |
| 70           | 15   |
| 75           | 14   |
| 80           | 12   |
| 85           | 11   |
| 90           | 9    |
| 95           | 7    |

### 3.3.3. Total heat transfer

The total heat transfer across the contact surface between the cold and the hot fluid over the length of the VT till the stagnation point will be,

$$\begin{aligned} \dot{Q}_{total} &= 2\pi k_t \int_8^{95} R_b(l)F(l)dl \text{ [Since for this model, inlet is at 15mm and stagnation point is at} \\ &\quad \text{95mm from cold end]} \\ &= (0.028) \int_8^{95} \{3.05 e^{-0.009l}\} \{65.038e^{-0.048l}\} dl \end{aligned}$$

$$\text{where, } 2\pi k_t = 2\pi(0.045) = 0.028 = 61.327\text{Watt}$$

It may be noted that the value of the total heat transfer obtained by the present analytical method is in good agreement with the total heat transfer value of 51.01 Watt obtained through CFD analysis for the same vortex tube of L/D = 30, by Behera et al. [5].

### 3.4. Generalization of total heat transfer in vortex tube

For the above two analysis, we have used an exponential function to approximate the function  $F(l)$ . Hence, the general form of  $F(l)$  can be rewritten as,

$$F(l) = Fe^{-\beta l} \quad (10)$$

Keeping the geometric and operating parameters constant except the length of the VT, we can derive the generalized heat transfer equation for different vortex tubes. Also, we will be to find out the dependence of constants such as  $R, \alpha, F$  and  $\beta$  on the length ( $L$ ) of the vortex tube.

Let's assume that  $R = r'L$ ,  $\alpha = \gamma L$ ,  $F = fL$ ,  $\beta = \delta L$ . Now, applying these constants to Eqs. (2) and (10), we get,

$$R_b(l) = r'Le^{-\gamma Ll} \quad (11)$$

and

$$F(l) = fLe^{-\delta Ll} \quad (12)$$

So the total heat transfer between the hot and the cold fluid can be expressed as,

$$\begin{aligned} \dot{Q}_{total} &= 2\pi k_t \int_0^{pL} \{r'Le^{-\gamma Ll}\} \{fLe^{-\delta Ll}\} dl \\ &= 2\pi k_t r' f L^2 \int_0^{pL} e^{-Ll(\gamma+\delta)} dl \\ &= 2\pi k_t r' f L^2 \left\{ \frac{e^{-Ll(\gamma+\delta)}}{-L(\gamma+\delta)} \right\} \Big|_0^{pL} \\ &= \frac{2\pi k_t r' f L^2}{L(\gamma+\delta)} (1 - e^{-pL^2(\gamma+\delta)}) \\ &= \frac{2\pi k_t r' f L}{(\gamma+\delta)} (1 - e^{-pL^2(\gamma+\delta)}) \end{aligned}$$

The above equation can be written as,

$$\dot{Q}_{Total} = ML (1 - e^{-NL^2}) \quad (13)$$

where,  $\frac{2\pi k_t r' f}{(\gamma+\delta)} = M$  and  $p(\gamma+\delta) = N$

From Eq. (13) we can find the maximum value of  $L$  i.e.  $L_{max}$  for which energy separation would be maximum for a particular diameter of the vortex tube.

## 4. Conclusion

- This novel analysis can calculate the precise value of heat energy transfer for any vortex tube.
- With additional data we can further calculate the value of the optimal length  $L_{max}$  for which energy separation inside the tube, would be maximum.

## References

- [1] G. J. Ranque, "Experiences sur la détente giratoire avec productions simulatanes d'un echappement d'air chaud et d'un echappement d'air froid," *J. Phys. Radium*, vol. 4, no. 7pp, pp. 112-114, 1993.

- [2] R. Hilsch, "The use of the expansion of gases in a centrifugal field as cooling process," *Rev. Sci. Instrum.*, vol. 18, no. 2, pp. 108–113, 1947. DOI: [10.1063/1.1740893](https://doi.org/10.1063/1.1740893).
- [3] T. Dutta, et al., "CFD Analysis of Energy Separation in Ranque - Hilsch Vortex Tube at Cryogenic Temperature," *J. Fluids*, vol. 2013, pp. 1–14, 2013., DOI: [10.1155/2013/562027](https://doi.org/10.1155/2013/562027).
- [4] U. Behera, et al., "CFD analysis and experimental investigation towards optimizing the parameters of Ranque – Hilsch vortex tube," *Int. J. Heat Mass Transf.*, vol. 48, no. 10, pp. 1961–1973, 2005. pp DOI: [10.1016/j.ijheatmasstransfer.2004.12.046](https://doi.org/10.1016/j.ijheatmasstransfer.2004.12.046).
- [5] U. Behera, et al., "Numerical investigations on flow behaviour and energy separation in Ranque – Hilsch vortex tube," *Int. J. Heat Mass Transf.*, vol. 51, no. 25-26, pp. 6077–6089, 2008., DOI: [10.1016/j.ijheatmasstransfer.2008.03.029](https://doi.org/10.1016/j.ijheatmasstransfer.2008.03.029).